Asian Journal of Chemistry; Vol. 32, No. 9 (2020), 2237-2242

ASIAN JOURNAL OF CHEMISTRY

https://doi.org/10.14233/ajchem.2020.22797

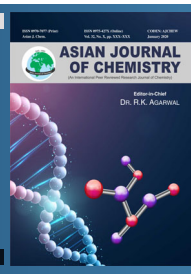

Behaviour of *ortho*-*N*-Glycoside as Green Corrosion Inhibitors for Tin in 0.5 M Citric Acid

MERVATE MOHAMED MOHAMED[1,3], FATIMA A. AL-QADRI[1,2], RAIEDHAH ALSAIARI[1], IMAN MOHAMMAD SHEDAIWA[1,2], MABKHOOT ALSAIARI[1] and ESRAA MOHAMED MUSA[1,4]

[1]Empty Quarter Research Centre, Department of Chemistry, Faculty of Sharourah's Science and Arts, Najran University, Sharourah, Saudi Arabia
[2]Department of Chemistry, Faculty of Science, Sana'a University, Sana'a, Yemen
[3]Department of Chemistry of Science faculty, Suez Canal University, Al Ismailia, Ismailia Governorate, Egypt
[4]Department of Biochemistry, Central Veterinary Research Labrotary, Khartoum, Sudan

*Corresponding author: E-mail: mmmohammad@nu.edu.sa

Received: 27 April 2020; *Accepted*: 30 May 2020; *Published online*: 20 August 2020; AJC-20019

A bio-nondegradable functional glycoside derivative, *viz. ortho*-*N*-glycoside, was extracted from natural cabbage plants and its corrosion inhibition behavior was evaluated in relation to tin in a 0.5 M citric solution. An electrochemical study, using potentiodynamic polarization and scanning electrochemical microscopy (SEM), was conducted to determine corrosion inhibition. The results indicate that *ortho*-*N*-glycoside possesses a corrosion inhibition efficiency of 75.83% at a concentration of 0.5 mol L^{-1}. The results of adsorption over the tin surface obeys Langmuir isotherm. The surface and the electrochemical reactivity of the tin samples in the citric acid solutions were examined using the SEM technique. This enable the corrosion type to be demonstrated. The results of the surface analysis be obtained using scanning electron microscopy (SEM).

Keywords: Weight loss, Acid corrosion, Adsorption models, Corrosion inhibitors, Cyclic voltammetry.

INTRODUCTION

In spite of all the improvements within the corrosion science and technology industries, corrosion is still a major issue for global industries. The cost of direct metal corrosion in the USA in 2002 was found to be around $ 276 billion per year, a much higher figure than the typical loss caused by natural disasters (which is $17 billion per year on average). Furthermore, it is possible to save about 25-30% of the cost of annual corrosion if the correct corrosion management processes are employed [1,2].

Inhibitor use is a primary practical technique that is employed to safeguard against corrosion, particularly in acidic solutions, since it can stop metal from being dissolved in the acid. It is simple to use inhibitors and they have the benefit of being able to be used promptly and without causing major disruption to the procedure. Being having the sufficient corrosion resistant property, tin often applied in the making of soft solders, dental amalgams, bronze and bottle cans [3]. Effective can packaging for is largely reliant upon the metal′s capacity to safeguard against corrosion. The corrosive resistance of the tinned plate is primarily determined by the metal′s key properties and the contents kept inside the can [4].

The level of corrosion caused in the tin when acidic fruits are placed inside has thus been the focus of increasing attention [5]. A majority of previous research has been concentrated on the inorganic anions for inhibiting the tin corrosion [6]. The use of such inorganic anions to inhibit corrosion is hindered by the toxicity that some of them are known to have. This, in addition to issues of sustainability and cost, have led to the corrosion inhibition habits of natural resources to warrant further investigation [7]. For example, there is a pH sensitive pigment in red cabbage leaves called anthocyanin, which is natural, cheap, readily available, safe and renewable [8]. The present research has the objective of exploring the potential use of red cabbage dye extract as an inhibitor for the corrosion of tin in citric acid solution using cyclic voltammetry and weight loss.

EXPERIMENTAL

ADPA tin sheets with high purity (99.5%) were used in this research. The reagents were procured from Zayo-Sigma

Chemicals Ltd. Analytical grade citric acid (purity < 99.9 %) was procured from Sigma-Aldrich, USA.

Preparation of *ortho-N*-glycoside from cabbage powder: Freshly purple cabbage purchased from the local market was washed thoroughly and sliced. All stems which contained less than the desired amount of pigment were subsequently discarded. The pink powder was obtained by air-drying the chopped cabbage at room temperature and then milling the leaves in a processor for 1 min. In this way, it was possible to obtain a homogeneous sample without risking the loss of any pigment content. Samples were placed in special containers for storage. After a period of 18 months, prepared *ortho-N*-glycoside (Fig. 1) was used to measure the corrosion inhibition, corrosion adsorption, adsorption thermodynamics and the kinetic effect on tin metal in citric acid at 30 ºC.

Preparation of 0.5 M citric acid: In order to prepare the acid solution of 0.5 M citric acid was diluted with distilled water. In addition, multiple inhibitor concentrations, ranging from 0.1 to 0.4% in weight, were added in the acid solution.

Cyclic voltammetry: A tin rod (A = 0.785 cm^2) was employed as the working electrode, while platinum (Pt) was utilized as the counter electrode and a silver chloride electrode (Ag/AgCl) was adopted as the reference electrode. Different grades of emery paper were used to polish the tin electrode prior to its immersion in deionized water for the rinsing stage. An X-Y recorder programmer, series 2000 Ominographic was connected to an EG & G Princeton Applied Research Potentiostat Galvanostat Model 263A in order to perform the cyclic voltammetry studies at room temperature (30 ºC). The pH of the solution was recorded with 1000 CE pH, mV and temperature meters.

Weight loss measurements: Tin sheets were cleaned, weighed and immersed in 50 mL of citric acid solution in the presence and absence of *ortho-N*-glycosides as inhibitors. Weight loss studies were performed at different time intervals with the recorded weight differences being assumed to equate to weight loss [9], which then employed to compute the corrosion rate associated with eqn. 1:

$$C = 10^4 \frac{ML}{\rho AT} \quad (1)$$

where ML = weight loss of the sheets, A = area of the sheet, ρ = density of tin metal and T = corrosion time.

The inhibition efficiency (IE%) was calculated [10] using eqn. 2:

$$IE\ (\%) = \frac{W_1 - W_0}{W_1} \times 100 \quad (2)$$

where W_0 and W_1 are the tin corrosion rates in the presence and absence of inhibitor, respectively in citric acid solutions. Surface coverage (θ) values were calculated using eqn. 3 [11]:

$$\theta = \frac{W_1 - W_0}{W_1} \quad (3)$$

SEM analysis: A scanning electron microscope (SEM) was utilized to record the microstructures of the surfaces of tin sheets following immersion. Different SEM magnifications were adopted, ranging from 100X to 12,000X by employing a secondary electron detector.

RESULTS AND DISCUSSION

Cyclic voltammetric studies: The effects of citric acid concentrates on tin from -1.5 to 1.5 V at a scan rate of 0.1 V s^{-1} at 30 ºC were explained by the cyclic voltammograms (Fig. 2). Hence, it can be observed that the density of cathodic current (I_c) decreases, thereby relocating the applied potential to less negative values before reaching zero at E_i = 0. Furthermore, E_i = 0 shifts were increased to more negative directions as the acid concentration increased. Meanwhile, the anodic current densities rise, as does the anodic potential. Table-1 presents the relationship between the corrosion current density for tin dissolution and the log c of the concentration of acid. The findings were indicative of the corrosion of tin immersed in citric acid being anodically controlled. In other words, that the corrosion of tin was hastened by the citrate ions. The reason was due to citrate ion adsorption on the surface of tin, where soluble Sn^{2+} and Sn^{4+} were both yielded and the hydrolysis of Sn^{4+} in citric acid results in the precipitation of $Sn(OH)_4$ and/or SnO_2 on the surface of tin (**Scheme-I**). In this way, the surface was rendered more passive [12-17].

TABLE-1
RELATION BETWEEN CITRIC ACID CONCENTRATION AND CORROSION PARAMETERS OF TIN AT 30 °C

Acid concentration (mol/L)	I_{corr} (μA/cm^2)	E_{corr} (mV)	Corrosion rate (mpy)
0.1	0.090	-348.8	0.0950
0.2	0.098	-248.7	0.1034
0.3	2.750	-198.7	2.9025
0.4	2.830	-148.6	2.9869
0.5	3.000	-98.6	3.1643

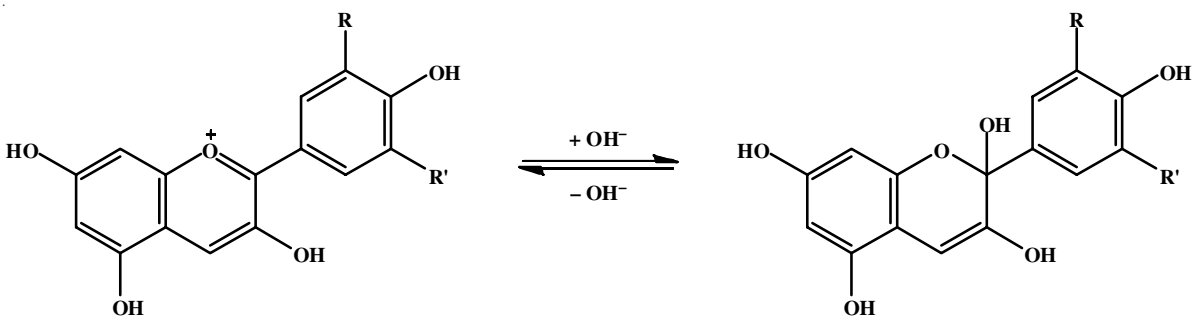

Fig. 1. Chemical structure of the *ortho*-N-glycosides

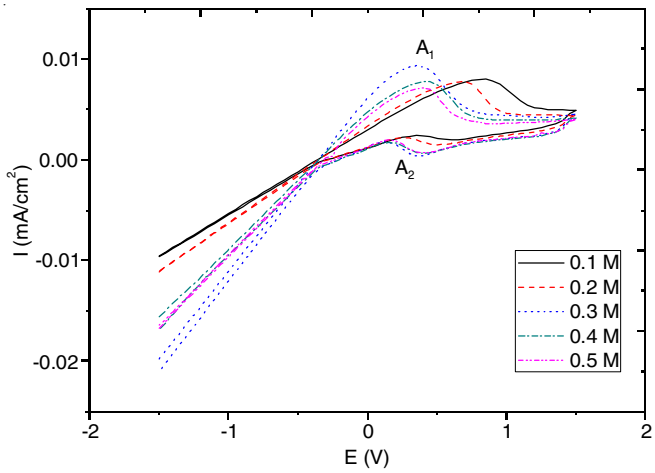

Fig. 2. Cyclic voltammetry curves for tin electrode at different concentrations of citric acid with scan rate of 0.1 V s^{-1} at 30 °C

$$Sn^{4+} + 4H_2O \longrightarrow Sn(OH)_4 + 4H^+$$
$$Sn(OH)_4 \longrightarrow SnO_2{\cdot}xH_2O + (2–x)H_2O$$

Scheme-I

Pitting corrosion caused a hysteresis loop to manifest in the cathodic direction [17]. The appearance of a minor anodic dissolution peak A_2 could be a consequence of the dissolution of metal *via* the passive film. Fig. 3 depicts the consequences of the elevated scan rate ν (0.1-0.5 V s^{-1}) on tin dissolution in 0.5 M citric acid (pH = 1.9) at 30 ºC. The curves suggest that increase in scan rate boost tin dissolution. Furthermore, Table-2 illustrates the relationship between the I_p of peaks A_1 and $\nu^{1/2}$, and revealed that the dissolution of tin in an anodic direction was an ordered process [18]. Moreover, with an increase in ν, the value of E_p becomes more noble and the passive film become less stable [19].

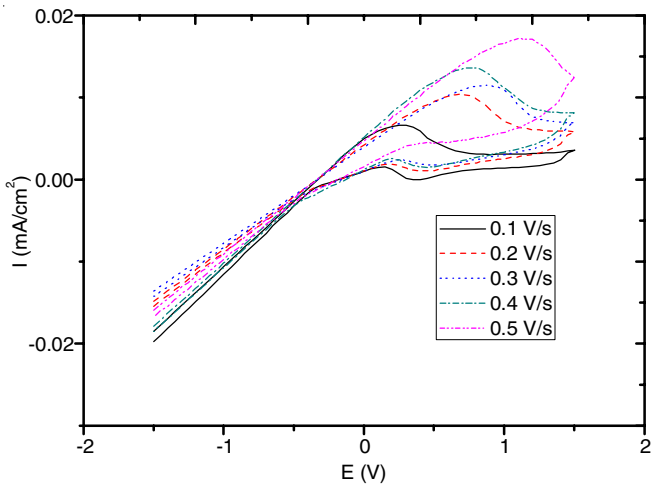

Fig. 3. Cyclic voltammetry curves for tin electrode at different scan rate of 0.5 M citric acid at 30 °C

Fig. 4 presents the impact on tin corrosion of the addition of *ortho-N*-glycosides in 0.5 M of citric acid at 30 ºC with a potential range from -1.5 to 1.5 V. These findings suggest increase in *ortho-N*-glycosides coincide with decreases in I_p and

TABLE-2
RELATION BETWEEN I_p AND $\nu^{1/2}$ FOR TIN IN 0.5 M CITRIC ACID AT 30 °C

$\nu^{1/2}$ (mV/s)$^{1/2}$	I_{diss} (μA/cm^2)	E_{diss} (mV)
0.1	6.68	251.77
0.2	10.38	702.21
0.3	11.49	852.36
0.4	13.63	802.31
0.5	17.16	1102.6

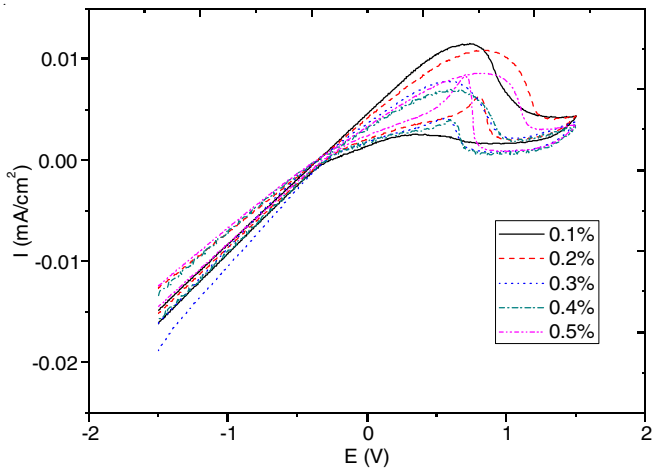

Fig. 4. Cyclic voltammetry curves for tin electrode at different concentration of inhibitor in 0.5 M citric acid at 30 °C

the shifting of E_p to a more negative direction. This generates a powerful inhibition impact on *ortho-N*-glycosides. Tin surface was blocked by the absorbing inhibitor, which hinders the adsorption of citrate anions.

Table-3 illustrates the relationship between inhibitor concentration and dissolution current densities wherein the data suggests that by raising *ortho-N*-glycoside concentration, it is possible to extend the inhibitory impact.

TABLE-3
RELATION BETWEEN INHIBITOR CONCENTRATION AND DISSOLUTION CURRENT DENSITIES FOR TIN IN 0.5 M CITRIC ACID AT 30 °C

$C_{inhib.}$ (%)	I_{diss} (μA/cm^2)	E_{diss} (mV)	Corrosion rate (mpy)
0.1	11.51	737.61	3.410
0.2	10.86	838.78	3.070
0.3	7.79	588.84	2.770
0.4	6.99	576.93	2.195
0.5	8.60	850.68	2.540

Weight loss measurements: Table-4 shows the increased weight loss associated with citric acid and extended exposure at 30 ºC, respectively. Also, data illustrates increasing of CR with both factors. Considering the corrosion rate, CR (mpy) and inhibition efficiency, IE%, as functions of the concentration in the citric acid, solutions were calculated using eqns. 1 and 2.

Table-5 illustrated that by increasing *ortho-N*-glycoside extract concentration from 0.1% to 0.5% by weight, it becomes possible to decrease weight loss in tin sheets. Hence, it can be deduced that *ortho-N*-glycoside effectively impedes tin corrosion. Data depicts the relationship between the IE% and the

TABLE-4
VARIATION OF WEIGHT LOSS WITH ACID CONCENTRATION AND EXPOSURE TIME FOR TIN SHEETS AT 30 °C

Acid conc. (mol/L)	Weight loss (mg)	Corrosion rate (mpy)	Time (h)	Weight loss (mg)	Corrosion rate (mpy)
0.1	7	149.96	0.5	7	456.57
0.2	13	278.49	1.0	7	228.28
0.3	14	299.91	1.5	17	369.60
0.4	14.5	310.63	2.0	24	391.34
0.5	15	321.34	2.5	22	286.98

TABLE-5
EFFECT OF INHIBITOR IN 0.5 M CITRIC ACID AT 30 °C FOR 1 h

Concentration (%)	Weight loss (mg)	Corrosion rate (mpy)	IE (%)	Surface coverage (θ)
Blank	24	782.68	–	–
0.1	23	750.07	4.167	0.04167
0.2	20	652.24	16.67	0.1667
0.3	10	324.89	58.33	0.5833
0.4	7	228.28	70.83	0.7083
0.5	7	228.28	70.83	0.7083

ortho-N-glycoside concentration in 0.5 M citric acid solution at 30 ºC, wherein increasing IE% for *ortho-N*-glycoside inhibitor with increasing *ortho-N*-glycoside. This suggests that the IE% comprises a function of the concentration of inhibitor present in the solution and the area of tin surface, which is covered with the absorbed inhibitors.

SEM analysis: Fig. 5 comprises an SEM image of tin sheet after 1 h immersion in 0.5 M citric acid solution. It can be seen that pits have appeared on surface of tin. This corrosion has occurred as a consequence of adsorption and penetration of citrate anions *via* the surface of tin.

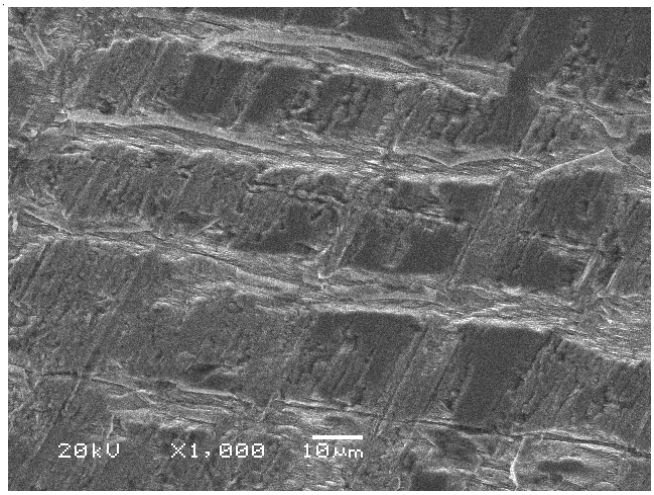

Fig. 5. SEM microphotograph for tin surface after immersion in 0.5 M citric acid for 1 h

Adsorption isotherms: The activation parameters resulted from absorption isotherms described the interaction of molecules on the surface of the electrode can be explained by the activation parameters, which arise from the absorption isotherms [20,21]. Thus different adsorption isotherms were tested in order to obtain more information about the interaction between the inhibitor and the tin metal surface. Various isotherms *viz.* El-Awady, Freundlich and Langmuir adsorption isotherms and linear regression coefficients (R^2) were used to determine the best fit. Only Langmuir adsorption isotherm (eqn. 4) was found to be best fit in which case all the linear regression coefficients (R^2) were close to unity (Fig. 6), where correlation coefficients (R^2) found to be 0.9984.

$$C/\theta = 1/K_{ads} + C \quad (4)$$

where θ = surface coverage, K_{ads} = Langmuir adsorption constant.

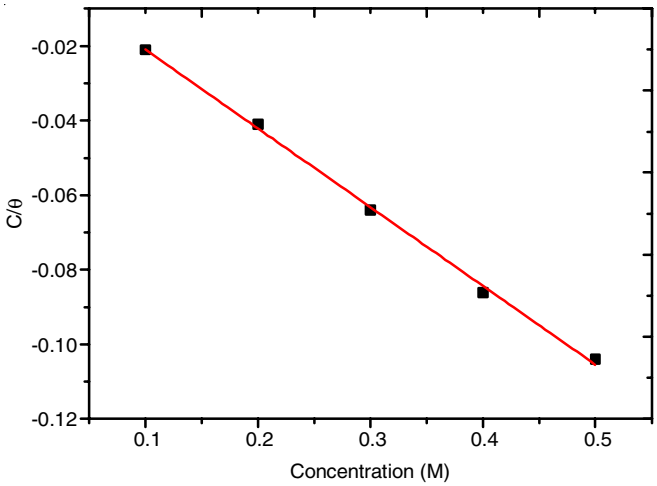

Fig. 6. Langmuir adsorption isotherm with citric acid solutions

In present case, *ortho-N*-glycoside shows the inhibition behaviour on the surface of corroded metals through a process of adsorption [22-24]. Furthermore, in order to facilitate absorption on the surface of metals, the green inhibitor incorporates physical properties, such as functional groups, aromaticity, steric effects, and the electron density of donor atoms [25,26].

Langmuir adsorption isotherm assumes that the solid surface contains a fixed number of adsorption sites and each site holds one adsorbed species. The equilibrium constant for the adsorption process (K_{ads}) is related to the standard Gibbs free energy of adsorption (ΔG_{ads}) by the following equation:

$$K_{ads} = \frac{1}{55.5e} - \Delta G_{ads} \quad (5)$$

where K_{ads} is the adsorption capacity and its values are shown in Table-6.

Thermodynamic analysis: Any investigation pertaining to the mechanisms of inhibition on the corrosion of metals must employ thermodynamic parameters [22,24]. The coefficient of correlation R^2, gave the degree of fit between the experimental data and the isotherm equation. The equilibrium constant for the adsorption capacity (K_{ads}) is related to the standard Gibbs free energy of adsorption (ΔG_{ads}) by the following equation [27,28]:

$$\Delta G_{ads} = -RT \ln (55.5\ K_{ads}) \quad (6)$$

The negative value of ΔG_{ads} indicated that the adsorption process is both spontaneous and stable on the surface of the tin layer [29,30]. The activation value ΔG_{ads} was -6.07, which

TABLE-6
ADSORPTION CAPACITY (K_{ads}) FROM SURFACE COVERAGE VALUE RESULTED FROM WEIGHT LOSS OF TIN AND FREE ENERGY OF ADSORPTION (ΔG_{ads}) OF VARIOUS LINE ARISED ISOTHERMS AT 24 °C BY USING DIFFERENT CONCENTRATION OF CITRIC ACID

Isotherm	Surface coverage θ					System	K_{ads}	ΔG_o ads (KJ/mol)
Langmuir	0.0050	0.0040	0.0020	0.0017	0.0014	0.5 M	-0.211	-6.07

TABLE-7
THERMODYNAMIC PARAMETERS FOR *ortho-N*-GLYCOSIDE (ONG) ADSORPTION ON TIN IN 0.5 M CITRIC ACID SOLUTIONS

System	Temperature (°C)	Adsorption models	ΔG_{ads} (kJ mol^{-1})	ΔH_{ads} (kJ mol^{-1})	E_a (kJmol^{-1})	ΔS_{ads} (kJ mol^{-1})
0.5 M	30	Langmuir	-6.07	-17.88	-23.58	-0.0192

regarded the adsorption process as physisorption, where the inhibition acted due to the electrostatic interaction between the charged molecules and the charged metal.

The negative values of heat contents (ΔH_{ads}) of tin in the citric acid, which means that the dissolution process is an exothermic phenomenon. Similarly, negative value of ΔS_{ads}, imply that the activated complex in the rate determining step represents an association rather than a dissociation step, meaning that a less disorder in the adsorption process.

Activation energy: *ortho-N*-glycoside inhibitor is found to increase the activation energy (E_a) value (Table-7), which indicates that the physisorption generates electrostatic attraction in the first stage of adsorption process. This can be attributed to the fact that higher values of E_a in the presence of inhibitor is due to the charge sharing or transfer from the organic inhibitor to the metal surface to form coordinate covalent bonds. The increase in E_a can be attributed to an appreciable decrease in the adsorption of the inhibitor on the steel surface with increase in temperature and a corresponding increase in corrosion rates occurs due to the fact that greater area of metal is exposed to solution.

Adsorption kinetics: The kinetic study of adsorption of corrosion inhibitor was evaluated by using eqn. 7 [23]:

$$\ln C_{corr} = \ln K + A \ln C_{inh} \quad (7)$$

where A is the reaction constant, C_{inh} is the concentration of the inhibitor in g/L and K is the rate constant.

Moreover, the half-life of adsorption was calculated using the following eqn. 8.

Half-life expression:

$$t_{1/2} = \frac{0.693}{k_t} \quad (8)$$

The rate constant parameters; rate constant and half-life are also recorded in Table-8. The plots showed a linear variation and slope k (figure not shown), which confirms a pseudo-first order reaction kinetics with respect to the corrosion of tin in 0.5 N citric acid solution in the absence and presence of *ortho-N*-glycoside. Table-5 also presents the half-life magnitude, wherein the lower values use *ortho-N*-glycoside at 30 ºC, thereby suggested that effectiveness of *ortho-N*-glycoside as corrosion inhibitor. Moreover, the value of reduced corrosion in tin is much better as compared to previous research [28].

TABLE-8
KINETIC PARAMETERS FOR (ONG) *ortho*-N-GLYCOSIDES ADSORPTION

System	Half-life $t_{1/2}$	Rate constant (K)	Reaction rate
0.5 M	77	0.0091	0.0269

Conclusion

The corrosion behaviour of tin in citric solution in the absence and presence of inhibitors was studied using cyclic voltammetry and weight loss methods under optimized conditions. *ortho-N*-glycoside is an effective inhibitor of tin corrosion in 0.5 M citric acid solutions. Increasing the concentration of *ortho-N*-glycoside renders it more effective, which is indicated by increasing the inhibition efficiency. The utilization of *ortho-N*-glycoside obyed the satisfactory results for all adsorption isotherm models. The kinetic study also revealed that equilibrium constant, rate constant, reaction rate and the $t_{1/2}$ of *ortho-N*-glycoside inhibitor can be considered as better corrosion inhibitior for tin.

CONFLICT OF INTEREST

The authors declare that there is no conflict of interests regarding the publication of this article.

REFERENCES

1. A. Rustandi and M.A. Barrinaya, *Appl. Mech. Mater.*, **842**, 24 (2016); https://doi.org/10.4028/www.scientific.net/AMM.842.24
2. G.H. Koch, Corrosion Costs and Preventive Strategies in the United States, US: NACE International (2002).
3. B.F. Giannetti, P.T.A. Sumodjo, T. Rabockai, A.M. Souza and J. Barboza, *Electrochim. Acta*, **37**, 143 (1992); https://doi.org/10.1016/0013-4686(92)80023-F
4. V.K. Gouda, E.N. Rizkalla, S. Abd El Wahab and E.M. Ibrahim, *Corros. Sci.*, **21**, 1 (1981); https://doi.org/10.1016/0010-938X(81)90058-5
5. N.A.-G. Abdel-Rahman, *J. Global Biosci.*, **4**, 2966 (2015).
6. S.S. Abdel Rehim, S.M. Sayyah and M.M. El Deeb, *Mater. Chem. Phys.*, **80**, 696 (2003); https://doi.org/10.1016/S0254-0584(03)00128-7
7. G. McKay, S.J. Allen, I.F. McConvey and M.S. Otterburn, *J. Colloid Interface Sci.*, **80**, 323 (1981); https://doi.org/10.1016/0021-9797(81)90192-2
8. P.K. Malik, *Dyes Pigments*, **56**, 239 (2003); https://doi.org/10.1016/S0143-7208(02)00159-6

9. A. S. Afolabi, A. C. Muhirwa, A. S Abdulkareem and E. Muzenda, *Int. J. Electrochem. Sci.*, **9**, 5895 (2014).
10. K.O. Orubite and N.C. Oforka, *Mater. Lett.*, **58**, 1768 (2004); https://doi.org/10.1016/j.matlet.2003.11.030
11. N.J.N. Nnaji, C.O.B. Okoye, N.O. Obi-Egbedi, M.A. Ezeokonkwo and J.U. Ani, *Int. J. Electrochem. Sci.*, **8**, 1735 (2013).
12. S.S. Abd El Rehim, A.M. Zaky and N.F. Mohamed, *J. Alloys Compd.*, **424**, 88 (2006); https://doi.org/10.1016/j.jallcom.2005.12.080
13. S.S. Abd El Rehim, H.H. Hassan and N.F. Mohamed, *Corros. Sci.*, **46**, 1071 (2004); https://doi.org/10.1016/S0010-938X(03)00134-3
14. C.M.V.B. Almeida, T. Rabóczkay and B.F. Giannetti, *J. Appl. Electrochem.*, **29**, 123 (1999); https://doi.org/10.1023/A:1003468731553
15. A. El-Sayed, F. Assaf and S.S. Abd El-Rehim, *Hung. J. Ind. Chem.*, **19**, 207 (1991).
16. N.F. El Boraei and S.S. Abd El Rehim, *Mater. Chem. Phys.*, **215**, 332 (2018); https://doi.org/10.1016/j.matchemphys.2018.05.040
17. R.M. El Sherif and W.A. Badawy, *Int. J. Electrochem. Sci.*, **6**, 6469 (2011).
18. M. Elboujdaini, E. Ghali, R.G. Barradas and M. Girgis, *Corros. Sci.*, **30**, 855 (1990); https://doi.org/10.1016/0010-938X(90)90009-T
19. H. Do Duc and P. Tissot, *Corros. Sci.*, **19**, 179 (1979); https://doi.org/10.1016/0010-938X(79)90016-7
20. E.A. Noor and A.H. Al-Moubaraki, *Mater. Chem. Phys.*, **110**, 145 (2008); https://doi.org/10.1016/j.matchemphys.2008.01.028
21. G. Avci, *Colloids Surf. A Physicochem. Eng. Asp.*, **317**, 730 (2008); https://doi.org/10.1016/j.colsurfa.2007.12.009
22. E.A. Noor, *Int. J. Electrochem. Sci.*, **2**, 996 (2007)
23. S.A. Abd El-Maksoud, *Int. J. Electrochem. Sci.*, **3**, 528 (2008).
24. I.B. Obot, N.O. Obi-Egbedi and S.A. Umoren, *Int. J. Electrochem. Sci.*, **4**, 863 (2009).
25. I. Langmuir, *J. Am. Chem. Soc.*, **38**, 2221 (1916); https://doi.org/10.1021/ja02268a002
26. A.K. Mishra and R. Balasubramaniam, *Mater. Chem. Phys.*, **103**, 385 (2007); https://doi.org/10.1016/j.matchemphys.2007.02.079
27. P.C. Okafor, U.J. Ekpe, E. Ebenso, E. Oguzie, N. Umo and A.R. Etor, *Trans. SAEST*, **41**, 82 (2006).
28. N.J.N. Nnaji, N.O. Obi-Egbedi and J.U. Ani, *J. Sci. Ind. Stud.*, **9**, 26 (2011).
29. N.O. Obi-Egbedi, K.E. Essien, and I.B. Obot, *J. Comput. Method Mol. Design*, **1**, 26 (2011).